Zinc-blende ZnO and its role in nucleating wurtzite tetrapods and twinned nanowires

Yong Ding and Zhong Lin Wang[a)]
School of Materials Science and Engineering, Georgia Institute of Technology, Atlanta, Georgia 30332-0245

Tianjun Sun and Jieshan Qiu
School of Chemical Engineering, Dalian University of Technology, Dalian 116012, China

(Received 1 February 2007; accepted 14 March 2007; published online 13 April 2007)

In this letter, the authors directly observed the zinc-blende (ZB) ZnO core in the initial formation of wurtzite (WZ) ZnO tetrapods. The formation of the wurtzite $(01\bar{1}3)$ twined nanowires is proposed based on the ZB core. Simple bonding density calculation shows that the wurtzite nanowires with $\{01\bar{1}0\}$ side surfaces have the lowest surface energy. A favorable choice of WZ phase over ZB when forming nanostructures is likely to be a result of surface energy minimization. This could be the reason that ZnS nanowires take WZ rather than ZB. © *2007 American Institute of Physics*. [DOI: 10.1063/1.2722671]

Nanowires and nanobelts of the most common semiconductors, such as ZnO, ZnS, CdSe, and CdS, can be synthesized by various techniques.[1–3] These materials can be cubic zinc blende (ZB) and hexagonal wurtzite (WZ), in which each atom is tetrahedrally coordinated by atoms of the opposite species.[4] The close-packed planes stack in *ABCABC* sequence in the ZB structure and *ABAB* in WZ structure.[5] The stability of WZ as compared to ZB is closely related to the deviation of the c/a lattice-parameter ratio from the ideal value of 1.633 for close-packed hexagonal.[6] Theoretical calculations[6–8] show that the Madelung constant for ideal WZ configuration is about 0.2% larger than that of ZB, so that the strong ionic compounds favor WZ. It is a well known fact that ZnO crystallizes in the WZ structure under normal pressure,[9] and the metastable ZB structured ZnO can be formed in epitaxial thin films,[10] but freestanding ZB nanostructures of ZnO, such as nanowires and nanobelts, have never been found.

The ZB phase has been found as the nucleus in the initiation of some nanostructures of ZnS, CdSe, CdS, and MnS,[11–15] but it is rather unstable and quickly transforms into the WZ phase once the crystal becomes bigger. The synthesis of ZnO tetrapods has been reported by many groups.[16–21] Three different growth mechanisms have been proposed about the formation of the ZnO tetrapods. One is based on the assumption of the existence of a ZB structured core at the center;[17] the second one is built upon the octahedral multiple twin structure;[19] the third one is that the ZB-type nucleus only exists in the high-temperature tetrapods and will degenerate to multiple twins after cooling down to room temperature.[18] Due to the lack of experimental evidence about the existence of ZnO ZB phased core, the tetrapod formation mechanism is still under debate.

In this work, by applying transmission electron microscopy (TEM), we give the direct experimental evidence of the existence of ZnO ZB core in our tetrapod nanoparticles. Based on the tetrapod structure, the polarization configuration of the wurtzite $(01\bar{1}3)$ twins has been proposed. Finally, we will explain the stability of the one-dimensional wurtzite nanostructures from the requirement of minimization of surface energy.

Tetrapod nanostructures have been found in ZnO, CdTe, CdS, ZnS, ZnSe, and CdSe.[11–21] TEM studies have directly given the evidence of the presence of ZB nucleus in the center of those tetrapod particles for all these materials except ZnO.[11–21] Due to the strongest ionic bonding of ZnO among the group, its most stable and most common phase is WZ. The only available evidence about the existence of ZB ZnO was derived from IR spectra.[22]

In the current study, the tetrapods were synthesized by a typical thermal vapor deposition process and were deposited on a polymer decorated Si substrate. The inset in Fig. 1(a) is a low-magnification TEM image of the ZnO tetrapods with each leg ~2 μm in length and 100–200 nm in width. The center part of the tetrapod is too thick to be clearly imaged by TEM. To overcome this problem, we have tried to examine the tetrapod with only two legs left. The bright-field and dark-field TEM images for such a case are displayed separately in Figs. 1(a) and 1(b). The selected-area electron diffraction pattern recorded from the two legs and connecting areas is displayed in Fig. 1(c). Besides two sets of well-defined WZ $[\bar{2}110]$ diffraction patterns, the extra diffraction spots can be uniquely indexed as the ZB [011] diffraction pattern. It is clear that the ZB phase does exist at the core of the ZnO tetrapod. If one of the WZ legs grew along the $[\bar{1}\bar{1}1]$ ZB axis, the second leg could be considered along the $[\bar{1}1\bar{1}]$ axis.

The existence of ZB core can be further confirmed by high-resolution TEM (HRTEM) image shown in Fig. 2, which was recorded from the leg intersecting area in Fig. 1(a). The size of the ZB core is around 30 nm. The matched plane between the ZB core and left WZ leg has been indexed as $(\bar{1}1\bar{1})\|(0001)$. The ZB core particle is a half octahedron. The two WZ legs grow epitaxially from the two triangle-shaped side surfaces of the ZB core. A sketch of the two-leg tetrapod is inserted in Fig. 2. The lattice distortion and stacking faults can be identified in the HRTEM image, which indicates a large strain located in the ZB core. The high density of stacking faults was produced due to a change

[a)]Author to whom correspondence should be addressed; electronic mail: zhong.wang@mse.gatech.edu

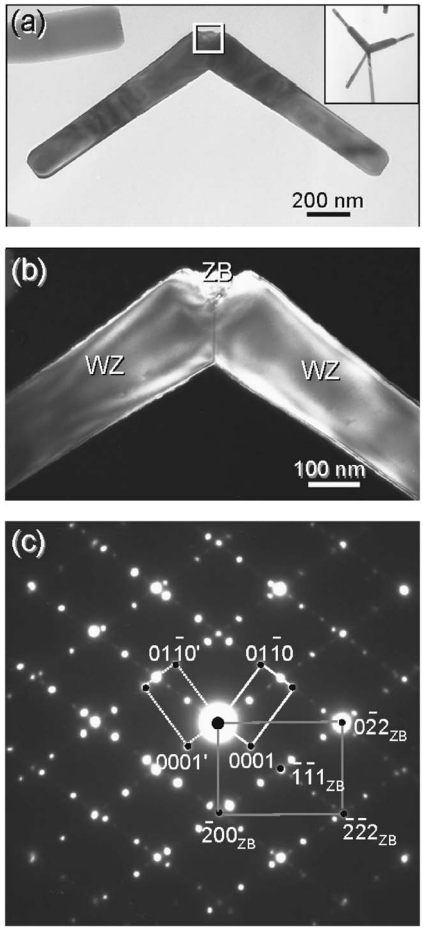

FIG. 1. (a) Bright-field and (b) dark-field TEM images of a two-legged ZnO tetrapod structure. The inset is a bright-field TEM image, showing a perfect ZnO tetrapod. (c) The selected-area electron diffraction pattern of the tetrapod in (a).

in stacking sequence from *ABC* to *AB* or *AC* during the phase transformation from ZB to WZ.

The existence of the ZB core indicates that, at least for the samples we are studying, the ZnO tetrapod can take a similar growth mechanism as that for CdTe, CdS, ZnS, ZnSe, CdSe, and MnS systems. A seed nucleates in ZB phase with an octahedral shape. The exposed eight surfaces can be classified into two groups with positive and negative charged ions exposed at the surfaces. Like in ZnO, the positive Zn^{2+} ion charged surfaces include (111), $(\bar{1}\bar{1}1)$, $(1\bar{1}\bar{1})$, and $(\bar{1}1\bar{1})$; their surface normal directions are shown in Fig. 3(a). The negative O^{2-} ion charged surfaces include $(\bar{1}\bar{1}\bar{1})$, $(11\bar{1})$, $(\bar{1}11)$, and $(1\bar{1}1)$. Figure 3(b) is the ZB atomic model projected along the [011] direction. If considering the dark-blue atoms as Zn and yellow atoms as O, the $(\bar{1}1\bar{1})$ and $(\bar{1}\bar{1}1)$ are Zn-terminated positively charged planes. Due to the self-catalysis effect of the cation-terminated surfaces,[23] the four positive charged surfaces can serve as the fast growth fronts to form the four legs of the tetrapod structure. It has been found that the legs of the tetrapods usually take WZ phase, which will be discussed toward the end.

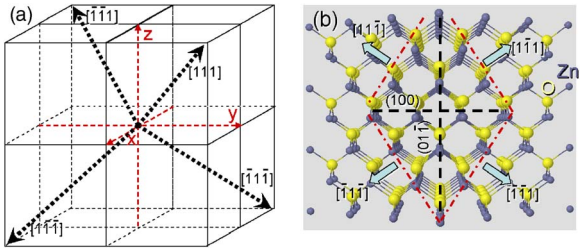

FIG. 3. (Color online) (a) Sketch of the four equivalent directions [111], $[\bar{1}\bar{1}1]$, $[1\bar{1}\bar{1}]$, and $[\bar{1}1\bar{1}]$ for the cubic ZB structures. (b) The atomic model of ZB structure projected along the [011] direction.

It is noticeable that the size of ZnO ZB core shown in Fig. 1 is just 1/4–1/5 of the width of the WZ legs. The two legs have a large contacted area at an angle of ~108°, which means that there is a higher energy interface between the two WZ legs. A small rotation between the two legs could lower the interface energy, and then a WZ twin structure may be formed. Figure 4 is a HRTEM image of a ZnO $(01\bar{1}3)$ twin structure.[24] The inset is the fast Fourier transform of the HRTEM image. The interface plane can be uniquely identified as $(01\bar{1}3)$. The *c* axis of the WZ ZnO is a polar direction, and the positive direction of the *c* axis is defined as the head and $-c$ is the tail. If we arbitrarily choose the positive *c* axis

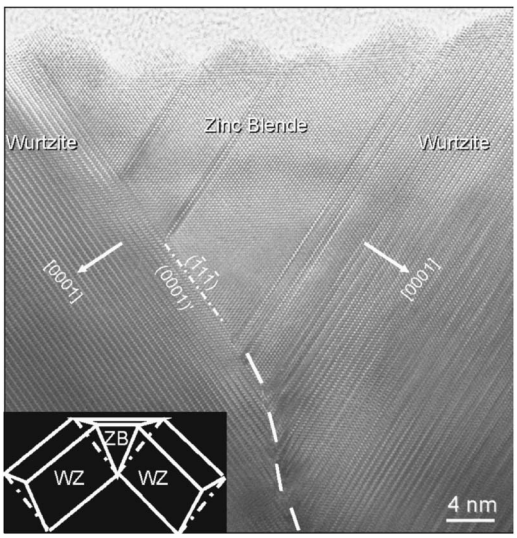

FIG. 2. The HRTEM image from the rectangle area in Fig. 1(a). The inset is a schematic model about the structure of the two-legged tetrapod.

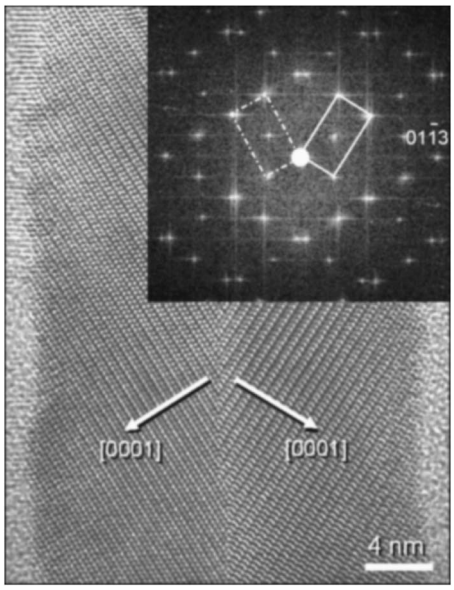

FIG. 4. HRTEM image of a $(01\bar{1}3)$ twin ZnO nanowire; the inset is the diffractogram of the HRTEM image.

TABLE I. Bond density at surfaces of zinc-blende and wurtzite structures ($d\sim$ the bond distance).

	Zinc blende		Wurtzite
{111}	$\sqrt{3}/(4d^2)\approx 0.433/d^2$	$\{01\bar{1}0\}$	$\sqrt{3}/(6d^2)\approx 0.459/d^2$
{100}	$3/(4d^2)\approx 0.750/d^2$	$\{\bar{2}110\}$	$3\sqrt{2}/(4d^2)\approx 1.061/d^2$
{110}	$3\sqrt{2}/(8d^2)\approx 0.530/d^2$	$\pm\{0001\}$	$\sqrt{3}/(4d^2)\approx 0.433/d^2$
{211}	$\sqrt{6}/(4d^2)\approx 0.612/d^2$		

on each side of the twin plane, we have three polarization configurations, head to head, tail to tail, and head to tail, whereas the head and tail directions correspond to the positive and negative c axes, respectively. The angle between the c axes of the two parts of the twin is around $\sim 116.7°$ (head to head and tail to tail) or 63.3° (head to tail). Looking back to Figs. 1 and 2 again, the fast growth direction of the legs is along the positive c axis. Therefore, it can be considered that the two legs of the broken tetrapod in Figs. 1 and 2 are in tail-to-tail configuration. The angle between the two legs is $\sim 108°$ as we measured from the diffraction pattern. Comparing the HRTEM images in Figs. 2 and 4, it is reasonable to choose the tail-to-tail configuration for the $(01\bar{1}3)$ twin structure. The two WZ legs of the tetrapod just need to rotate $\sim 9°$, and then the $(01\bar{1}3)$ conjugated plane for the $(01\bar{1}3)$ twin is a favorable interface of choice.

The most stable bulk form of ZnS at room temperature is the ZB structure, which can transfer to the metastable WZ structure after heating to 1020 °C in ambient pressure. In recent reported ZnS nanostructures, including nanowires, nanobelts/nanoribbons, nanosaws, and nanocables, the dominant phase is WZ.[25,26] Other materials such as CdSe, CdS, MnS, and GaN can be ZB or WZ in bulk forms, while their one-dimensional nanostructures prefer the WZ phase.[11–21] ZnO has exclusively taken the WZ structure when forming nanomaterials. To find a clue, we examine the surface structure of ZB and WZ phases.

It is considered that the surface contribution to the total energy becomes increasingly important as the size decreases. We try to reveal the WZ and ZB stability in one-dimensional nanostructure by investigating the difference in surface energy. The favorite growth direction of one-dimensional WZ nanostructures is along the c axis with exposed surface being $\{01\bar{1}0\}$ or $\{2\bar{1}\bar{1}0\}$. The c axis of WZ corresponds to the $\langle 111\rangle$ direction of ZB. If [111] is the growth direction for the ZB nanowire, the exposed surfaces would be {110} or {211).

For the nonpolar surfaces, the major contribution to the surface energy is the energy from the breaking bonds at the surface. We can roughly use the bond density of each surface to represent the surface energy.[5] The calculated results have been listed in Table I. d is the bonding distance between one atom and its three closest neighbors in opposite species. For simplicity, we take the WZ as an ideal case with $a/c=\sqrt{8/3}$ and u parameter (ratio of nearest-neighbor distance along the c axis to c) equal to 3/8.[27]. Except the polar surfaces $\pm(0001)_{WZ}/\{111\}_{ZB}$ and $\{100\}_{ZB}$, the lowest bond density surface is $\{01\bar{1}0\}_{WZ}$. The one-dimensional nanostructure growth along the [0001] direction with exposed $\{01\bar{1}0\}$ side surfaces is likely to have the lowest surface energy. This surface energy driven phase transformation is further enhanced with the increased surface-to-volume ratio. After the nucleation, the growth of the one-dimensional nanostructure along the stacking direction of close-packed plane will prefer the *ABAB* instead of the *ABCABC* sequence to expose the $\{01\bar{1}0\}$ side surfaces. As a conclusion, the comparable low surface energy of $\{01\bar{1}0\}$ plane takes the key role in stabilizing the wurtzite phase in one-dimensional nanostructures. This is likely the reason that the legs of the tetrapod are WZ rather than ZB. Our model here may also provide an explanation about the formation of the WZ phase nanostructures, especially for ZnS.

In summary, we directly observed the zinc-blende phased core in the ZnO tetrapod nanostructures, showing a direct evidence of the ZB core in the nucleation of the wurtzite tetrapod structure. The formation of the WZ $(01\bar{1}3)$ twinned nanowires is discussed based on the developed model. By calculating the bond density at the surfaces for both ZB and WZ structures, we find that the [0001] growth wurtzite nanowires with $\{01\bar{1}0\}$ side surfaces have the lowest surface energy.

[1] D. Moore and Z. L. Wang, J. Mater. Chem. **16**, 3898 (2006).
[2] Z. W. Pan, Z. R. Dai, and Z. L. Wang, Science **291**, 1947 (2001).
[3] L. Manna, D. J. Milliron, A. Meisel, E. C. Scher, and A. P. Allivisatos, Nat. Mater. **2**, 382 (2003).
[4] R. W. G. Wyckoff, *Crystal Structure*, 2nd ed. (Interscience, New York, 1963).
[5] W. A. Harrison, *Electronic Structure and the Properties of Solid* (Freeman, San Francisco, 1980), pp. 229–256.
[6] C. Y. Yeh, Z. W. Lu, S. Froyen, and A. Zunger, Phys. Rev. B **46**, 10086 (1992).
[7] C. Y. Yeh, S. H. Wei, and A. Zunger, Phys. Rev. B **50**, 2715 (1994).
[8] J. Serrano, A. H. Romero, F. J. Manjón, R. Lauck, M. Cardona, and A. Rubio, Phys. Rev. B **69**, 094306 (2004).
[9] G. D. Archard, Acta Crystallogr. **6**, 657 (1953).
[10] A. B. M. A. Ashrafi, A. Ueta, A. Avramescu, H. Kumano, I. Suemune, Y. W. Ok, and T. Y. Seong, Appl. Phys. Lett. **76**, 550 (2000).
[11] Y. W. Jun, Y. Y. Jung, and J. Cheon, J. Am. Chem. Soc. **124**, 615 (2002).
[12] D. J. Milliron, S. M. Hughes, Y. Cui, L. Manna, J. Li, L. W. Wang, and A. P. Allivisatos, Nature (London) **430**, 190 (2004).
[13] M. Chen, Y. Xie, J. Lu, Y. Xiong, S. Zhang, Y. Qian, and X. Liu, J. Mater. Chem. **12**, 748 (2002).
[14] J. Gong, S. Yang, H. Huang, J. Duan, H. Liu, X. Zhao, R. Zhang, and Y. Du, Small **2**, 732 (2006).
[15] Q. Pang, L. Zhao, Y. Cai, D. P. Nguyen, N. Regnault, N. Wang, S. Yang, W. Ge, R. Ferreira, G. Bastard, and J. Wang, Chem. Mater. **17**, 5263 (2005).
[16] M. L. Fuller, J. Appl. Phys. **15**, 164 (1944).
[17] M. Shiojiri and C. Kaito, J. Cryst. Growth **52**, 173 (1981).
[18] K. Nishio, T. Isshiki, M. Kitano, and M. Shiojiri, Philos. Mag. A **76**, 889 (1997).
[19] M. Fujii, H. Iwanaga, M. Ichihara, and S. Takeuch, J. Cryst. Growth **134**, 275 (1993).
[20] Y. Dai, Y. Zhang, and Z. L. Wang, Solid State Commun. **126**, 629 (2003).
[21] C. Ronning, N. G. Shang, I. Gerhards, H. Hofsäss, and M. Seibt, J. Appl. Phys. **98**, 034307 (2005).
[22] T. Tanigaki, S. Kimura, N. Tamura, and C. Kaito, Jpn. J. Appl. Phys., Part 1 **41**, 5529 (2002).
[23] Z. L. Wang, X. Y. Kong, and J. M. Zuo, Phys. Rev. Lett. **91**, 185502 (2003).
[24] Y. Ding and Z. L. Wang, J. Phys. Chem. B **108**, 12280 (2004).
[25] D. Moor, C. Ronning, C. Ma, and Z. L. Wang, Chem. Phys. Lett. **385**, 8 (2004).
[26] Y. Ding, X. D. Wang, and Z. L. Wang, Chem. Phys. Lett. **398**, 32 (2004).
[27] E. H. Kisi and M. M. Elcombe, Acta Crystallogr., Sect. C: Cryst. Struct. Commun. **C45**, 1867 (1989).